

1 We would like to thank all three reviewers for acknowledging our contributions and providing valuable feedback. Please  
 2 find our responses to your comments below.

3 **Reviewer #1:**

4 Thank you for the positive comments on the novelty of our idea and insightful questions for further improvement.  
 5 We first characterize the solutions of DEAN. Let  $p_x$  and  $p_{x'}$  be the distributions of real and fake data;  $p_e$  denotes the  
 6 energy-based distribution. In DEAN,  $p_e$  is a bridge connecting  $p_x$  and  $p_{x'}$ . Now we provide two theorems for the  
 7 characterization. For the IGN, the network is trained to have  $p_{x'}$  equal to  $p_e$ . Please refer to Theorem 1, which is proved  
 8 based on Theorem 1 of [JXS<sup>+</sup>17]. For the EGN,  $p_e$  is learned to estimate  $p_x$ . Please see Theorem 2, which is proved  
 9 according to Theorem 1 of [ZML17] and Theorem 1 of [GPAM<sup>+</sup>14]. At present, Theorem 2 is proved with  $\Lambda(\theta_e)$ .  
 10 Other choices for the energy objective will be left to future works. Detailed proofs of the following theorems will  
 11 be given in the Supplement of the final version. Different from GANs, which are implicit generative models (IGMs),  
 12 DEAN can explicitly estimate the underlying distribution of the real data after estimating  $\theta_e$  and  $\theta_g$ .

13 **Theorem 1** We assume that  $\mathcal{D}_{x'}$  is drawn from  $p_{x'}$ . If the following conditions are satisfied:  $\kappa$  is a universal and  
 14 analytic kernel;  $\mathbf{E}_{a \sim p_x} \mathbf{E}_{b \sim p_e} \left[ s^T(a) s(b) \kappa(a, b) + s^T(b) \nabla_a \kappa(a, b) + s^T(a) \nabla_b \kappa(a, b) + \sum_{i=1}^d \frac{\partial^2 \kappa(a, b)}{\partial a_i \partial b_i} \right] < \infty$  with  
 15  $s(a) = \nabla_a \log p_e(a)$ ;  $\mathbf{E}_{a \sim p_{x'}} \|\nabla_a \log p_e(a) - \nabla_a \log p_{x'}(a)\|^2 < \infty$ ;  $\lim_{\|a\| \rightarrow \infty} p_e(a) g(a) = 0$ , where  $g(\cdot)$  is given  
 16 in Eq. (2) in Section 4.2; for any  $J \geq 1$ , almost surely  $\text{FSSD}[p_e, \mathcal{D}_{x'}] = 0$  if and only if  $p_{x'} = p_e$ .

17 **Theorem 2** Let  $\Lambda(\theta_e) = \mathcal{E}(x; \theta_e) + [\gamma - \mathcal{E}(G(z; \theta_g^*); \theta_e)]^+$  (please refer to Eq. (1) in Section 4.1 for details). The  
 18 minimum of  $\Lambda(\theta_e)$  is achieved if and only if  $p_e = p_x$ . With the optimized  $\theta_e^*$ ,  $\int_{x,z} \Lambda(\theta_e^*) p_x(x) p_z(z) dx dz = \gamma$ .

19 Following your suggestion, we compare the powers (successful rejection rates) of MMD, linear-time MMD [GBR<sup>+</sup>12]  
 20 and FSSD on toy problems, where MMD is a two-sample test statistic and FSSD is used for the GOF test.

21 We adopt the distributions Gaussian  $p(x) = \mathcal{N}(x|0, \mathbf{I}_d)$  and  
 22 Laplacian  $q(x) = \prod_{i=1}^d \text{Laplace}(x_i|0, 1/\sqrt{2})$  for  $d = 1, 3$ , in  
 23 which the parameters are set to make  $p$  and  $q$  have the same mean  
 24 and variance so that the difference between  $p$  and  $q$  is subtle. F-  
 25 SSSD shows a higher power to discriminate the subtle difference  
 26 (Figure 1). For larger sample sizes, the power of MMD is close to  
 27 that of FSSD. However, in the GAN-type training, the batch size  
 28 is usually less than 512. As the adversarial training continues, the  
 29 distribution of the generated data gets closer to the energy-based  
 30 distribution, and hence the difference becomes subtle. At this  
 31 time, the power (discriminability) of FSSD for the subtle differ-  
 32 ence becomes important for generating high-quality images. Hopefully we have cleared up your main concerns with  
 33 these theoretical and experimental discussions. We believe that the DEAN paradigm is promising, being versatile to  
 34 yield specific training algorithms for different architectures of deep networks in different domains.

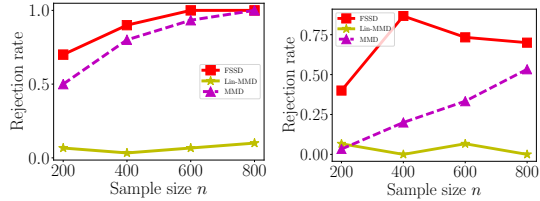


Figure 1: Rejection rates for  $d = 1$  (left) and  $d = 3$ .

35 **Reviewer #2:**

36 Thank you very much for the encouraging comments and valuable suggestions.  
 37 Following your recommendation, we will add more discussions in the experimental part to provide takeaways and  
 38 insights about DEAN. We adopted RBM as the energy function at the initial stage. However, the performance of DEAN  
 39 with RBM is not comparable to that with autoencoder, so we discarded the results. We will add clarity on this in the  
 40 final manuscript.

41 **Reviewer #3:**

42 Thank you very much for the positive comments and reasonable doubt.  
 43 In recent years, there are two emerging families for generative model learning, generative adversarial networks (GANs)  
 44 and autoencoders (AEs) or variational AEs (VAEs), which are two distinct paradigms and have both received extensive  
 45 studies. Goodness-of-fit (GOF) tests are a fundamental tool in statistical analysis, dating back to the Kolmogorov test in  
 46 1933. Our manuscript and [PDB18] both introduce GOF tests into deep generative modeling, but fall into different  
 47 paradigms: [PDB18] is an AE-based method without adversarial learning while our paper is a GAN-type approach. The  
 48 HTAE (hypothesis testing AE) in [PDB18] minimized the reconstruction error, but no adversarial learning (min-max  
 49 adversarial optimization) was involved. The statistic in our manuscript is a kernel-based *nonparametric* GOF statistic.  
 50 The Shapiro-Wilk test in [PDB18] is a traditional *parametric* GOF statistic for testing normality. Our paper is quite  
 51 different from [PDB18]. The proposed DEAN with two generators is a pioneering work in the adversarial learning  
 52 setting. Following your comment, we will cite [PDB18] in the final version.

53 **References**

54 [PDB18] Aaron Palmer, Dipak Dey, and Jinbo Bi. Reforming generative autoencoders via goodness-of-fit hypothesis testing. In  
 55 *UAI*, pages 1009–1019, 2018.